Dielectric dispersion on the Kerr constant of blue phase liquid crystals

Yan Li,[1] Yuan Chen,[1] Jie Sun,[1] Shin-Tson Wu,[1,a)] Shih-Hsien Liu,[2] Pao-Ju Hsieh,[2] Kung-Lung Cheng,[2] and Jyh-Wen Shiu[3]
[1]*College of Optics and Photonics, University of Central Florida, Orlando, Florida 32816, USA*
[2]*Material and Chemical Research Laboratories, Industrial Technology Research Institute, Hsinchu, Taiwan*
[3]*Display Technology Center, Industrial Technology Research Institute, Hsinchu, Taiwan*

(Received 27 September 2011; accepted 12 October 2011; published online 4 November 2011)

Dielectric dispersions on the Kerr constant of two polymer-stabilized blue phase liquid crystals (BPLCs) are investigated. An *extended Cole-Cole model* is proposed to fit the experimental results and good agreement is obtained. As the electric field frequency increases, Kerr constant decreases and the associated dielectric heating effect gradually increases. These results will undoubtedly affect the high frequency operation of BPLC devices. © *2011 American Institute of Physics*. [doi:10.1063/1.3657768]

Polymer-stabilized blue phase liquid crystal (BPLC)[1–5] is promising for next-generation display and photonics applications because it exhibits following attractive features: optically isotropic dark state, no need for surface alignment layer, and submillisecond gray-to-gray response time.[6] Especially fast response time is critically needed for a wide range of photonics applications, such as laser beam steering and adaptive optics,[7] polarization independent adaptive lens,[8] switchable phase grating,[9] and color sequential displays.[10,11] However, the high operating rate on BPLC devices requires high frequency of AC electric fields to avoid ionic effect. Therefore, frequency effect of BPLCs is of practical importance.

The physical mechanism of a polymer-stabilized BPLC is governed by electric-field-induced birefringence through Kerr effect. However, Kerr effect is valid only in the weak field region. As the electric field (E) increases, the induced birefringence gradually saturates following extended Kerr model as:[12]

$$\Delta n_{ind}(E) = \Delta n_s[1 - \exp(-(E/E_s)^2], \quad (1)$$

where Δn_s is the saturation induced birefringence and E_s is the saturation electric field. The optical dispersion of Kerr constant has been studied[13] and the Kerr constant is found to decrease with wavelength. But the dielectric dispersion of Kerr constant in BPLCs remains unexplored. Therefore, there is an urgent need to investigate the frequency effects on the Kerr constant of BPLC devices.

In this paper, we report the electric field frequency effects on the Kerr constant of two polymer-stabilized BPLCs and fit our experimental results with the extended Cole-Cole equation. Good agreement is obtained. As the electric field frequency increases, Kerr constant decreases and the associated dielectric heating gradually increases.

In our experiment, we prepared two in-plane-switching (IPS) cells whose electrode width and electrode gap are both 10 μm and cell gap is 7.5 μm. Cell 1 was filled with a BPLC mixture consisting of 76.2 wt. % JM2069-043 nematic LC host (from ITRI), 13 wt. % chiral dopants [8% ISO-(6OBA)$_2$ and 5% CB15 (Merck)], 10 wt. % monomers [6% RM257 (Merck) and 4% 1,1,1-Trimethylolpropane Triacrylate (TMPTA, Sigma Aldrich)], and ~0.8 wt. % photoinitiator. The cell was cooled to BP-I phase and the precursor was cured by an UV light with $\lambda \sim 365$ nm and intensity ~2 mW/cm^2 for 30 min. After UV curing, the polymer-stabilized BPLC composite was self-assembled, and the clearing temperature was measured to be $T_c \sim 44\,^\circ$C. The relatively low T_c is attributed to the low melting point (~4 °C) of the chiral dopant CB-15. Cell 2 was filled with Chisso JC-BP01M precursor, in which chiral dopant and monomers were premixed. The UV curing conditions were the same as reported in Ref. 14, and the T_c of sample 2 is ~70 °C.

Next, we measured the voltage-dependent transmittance (VT) curves of these two cells using a He-Ne laser ($\lambda = 633$ nm). The cells were placed in a temperature controller to have a constant temperature ~22 °C. Figure 1 shows the normalized VT curves of cell 1 at five frequencies: 100, 1, 10, 50, and 100 kHz. As frequency increases, the VT curve shifts rightward, indicating that the on-state voltage (V_{on}) increases (i.e., Kerr constant decreases) with frequency.

We fitted the VT curves shown in Fig. 1 with Eq. (1) at each frequency. In our experiment, we used the same probing wavelength but changing the electric field frequency. Thus during fittings we kept $\Delta n_s = 0.19$ and only changed E_s for different frequencies. Once Δn_s and E_s are obtained, we

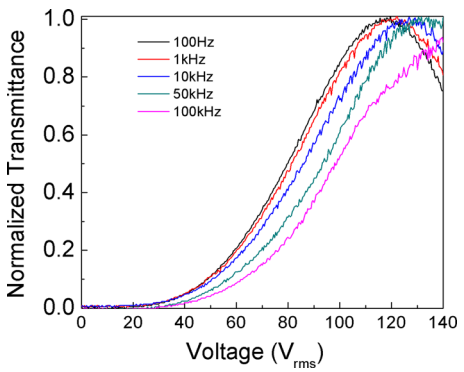

FIG. 1. (Color online) Measured VT curves of sample 1 at different frequencies.

a)Electronic mail: swu@mail.ucf.edu.

then calculate Kerr constant $K = \Delta n_s/(\lambda E_s^2)$ through extended Kerr model. In Fig. 2, we plot the obtained frequency dependent Kerr constant (red closed circles) at logarithmic scale.

On the theory side, Gerber found that Kerr constant can be approximated by the following equation:[15]

$$K \approx \Delta n \Delta\varepsilon \frac{p^2}{k\lambda(2\pi)^2}, \tag{2}$$

where Δn is the birefringence, $\Delta\varepsilon$ is the dielectric anisotropy, and k is the elastic constant of the host LC, respectively, and p is the pitch length. Among all the parameters in Eq. (2), only $\Delta\varepsilon$ is related to the electric field frequency. Therefore, Kerr constant and $\Delta\varepsilon$ should have the same frequency effect.

To prove this, we also include the measured dielectric anisotropy of host LC (black open circles) in Fig. 2 but using a different scale. As expected, the frequency dependent K and $\Delta\varepsilon$ curves overlap quite well, indicating that K is indeed proportional to $\Delta\varepsilon$ as Eq. (2) predicts.

For a LC mixture, the frequency dependent dielectric constants $\varepsilon_{//}$ and $\varepsilon_\perp$ can be described by the following Cole-Cole equation:[16]

$$\varepsilon^*(f) = \varepsilon_\infty + \frac{\varepsilon_s - \varepsilon_\infty}{1 + (i\frac{f}{f_r})^{1-\alpha}}, \tag{3}$$

where $\varepsilon^* = \varepsilon' + i\varepsilon''$ is the complex dielectric constant at frequency f, ε_s and ε_∞ are the dielectric constants at static and high frequencies, respectively, f_r is the relaxation frequency, i is the imaginary unit, and α is a value between 0 and 1, which allows to describe different spectral shapes. The real part of the complex dielectric constant (ε') is the one we commonly measure ($\varepsilon_{//}$ and $\varepsilon_\perp$), and the imaginary part (ε'') is responsible for the dielectric heating.

For a rod-like compound, $\varepsilon_\perp$ has a much higher relaxation frequency than $\varepsilon_{//}$ due to its shorter dipole length in the direction perpendicular to molecular axis.[17] Thus in the low frequency region, the relaxation of $\varepsilon_{//}$ as described by the real part of Cole-Cole equation is noticeable, while $\varepsilon_\perp$ remains unchanged ($\varepsilon_\perp = \varepsilon_{\perp s}$). As a result, dielectric anisotropy ($\Delta\varepsilon = \varepsilon_{//} - \varepsilon_\perp$) also follows the real part of Cole-Cole equation, i.e., it has the same relaxation frequency as $\varepsilon_{//}$:

$$\Delta\varepsilon(f) = \Delta\varepsilon_\infty + (\Delta\varepsilon_s - \Delta\varepsilon_\infty)\frac{1 + (\frac{f}{f_r})^{1-\alpha}\sin\frac{1}{2}\alpha\pi}{1 + 2(\frac{f}{f_r})^{1-\alpha}\sin\frac{1}{2}\alpha\pi + (\frac{f}{f_r})^{2(1-\alpha)}}, \tag{4}$$

where $f_r = f_{r//}$, $\Delta\varepsilon_\infty = \varepsilon_{//\infty} - \varepsilon_{\perp s}$, $\Delta\varepsilon_s = \varepsilon_{//s} - \varepsilon_{\perp s}$, $\Delta\varepsilon_s$ is the static dielectric anisotropy, and $\Delta\varepsilon_\infty$ is the dielectric anisotropy in the high frequency region.

Since Kerr constant is linearly proportional to $\Delta\varepsilon$ as Eq. (2) shows, we can modify Eq. (4) to describe the frequency dependent Kerr constant as

$$K(f) = K_\infty + (K_s - K_\infty)\frac{1 + (\frac{f}{f_r})^{1-\alpha}\sin\frac{1}{2}\alpha\pi}{1 + 2(\frac{f}{f_r})^{1-\alpha}\sin\frac{1}{2}\alpha\pi + (\frac{f}{f_r})^{2(1-\alpha)}}, \tag{5}$$

where K_s and K_∞ stand for the Kerr constant at static and high frequency, respectively. For convenience, we call Eq. (5) as *extended Cole-Cole equation*.

While comparing model with experimental data, we first use Eq. (3) to fit the real and imaginary parts of $\varepsilon_{//}$, respectively and obtain $\varepsilon_{//\infty}$, $\varepsilon_{//s}$, f_r, and α. In the low frequency region, $\varepsilon_{//s}$ is insensitive to frequency and can be treated as constant. The remaining three parameters are fairly unique because we have to fit two curves simultaneously. Next, we use Eq. (4) to fit the measured frequency dependent $\Delta\varepsilon$ of sample 1 and results are plotted in Fig. 2. Afterwards, we scale $\Delta\varepsilon_\infty$ and $\Delta\varepsilon_s$ to K_∞ and K_s to fit Kerr constant (Eq. (5)) because K is linearly proportional to $\Delta\varepsilon$ as Eq. (2) shows. The parameters of sample 1 are $K_s = 1.48\,\text{nm/V}^2$, $K_\infty = -0.189\,\text{nm/V}^2$, $f_r = 118\,\text{kHz}$, and $\alpha = 0.12$. The negative K_∞ indicates there is a crossover frequency for Kerr constant. This is not uncommon for some LC compounds whose $\Delta\varepsilon$ turns to negative in high frequency region.[17,18] As Fig. 2 shows, the fitted curve (pink solid line) agrees very well with the experimental data.

For sample 2 (Chisso JC-BP01M), we also measured its VT curves at different frequencies. Results are plotted in Fig. 3. From Fig. 3, the VT curves gradually shift to the right side and V_{on} increases as frequency increases. At 5 kHz, the transmittance at 60V_{rms} is only ~10% of that of the peak transmittance. These results indicate that frequency has a tremendous impact on the electro-optic properties of the BPLC cell.

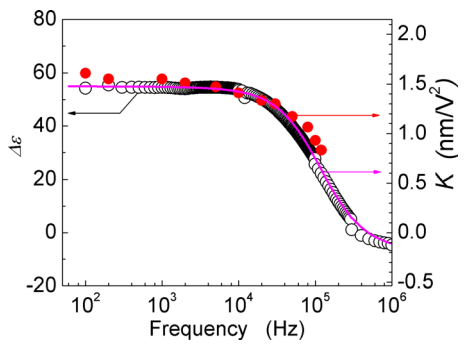

FIG. 2. (Color online) Kerr constant and $\Delta\varepsilon$ versus frequency for BPLC sample 1. Black open circles are $\Delta\varepsilon$, red filled circles are Kerr constant obtained from VT curves, and pink solid line is the fitting of Kerr constant using Eq. (5) with $K_\infty = -0.189\,\text{nm/V}^2$, $f_r = 118\,\text{kHz}$, and $\alpha = 0.12$.

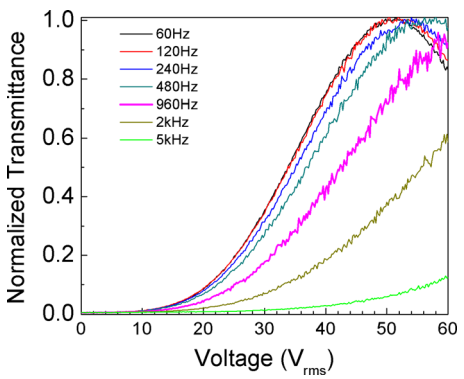

FIG. 3. (Color online) Measured VT curves of sample 2 at different frequencies.

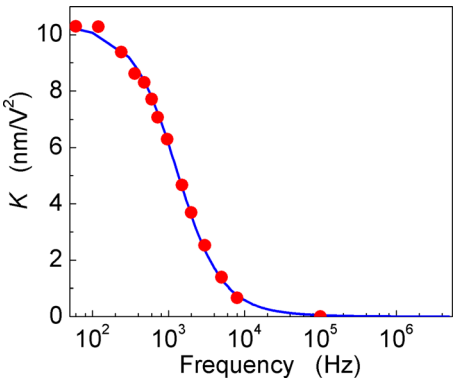

FIG. 4. (Color online) Kerr constant versus frequency for BPLC sample 2 (Chisso JC-BP01M). Red filled circles are Kerr constant obtained from VT curves, and blue curve is the fitting of Kerr constant Eq. (5) with $K_\infty = 0$, $f_r = 1300$ Hz, and $\alpha = 0.13$.

We used similar procedures to fit the measured VT curves (Fig. 3) with extended Kerr model. Here the saturation birefringence $\Delta n_s = 0.15$ and $K_s = 10.4\,\text{nm}/V^2$. Figure 4 shows the frequency dependent Kerr constant of Chisso JC-BP01M; the red circles are experimental data and solid line denotes fitting using Eq. (5) with $K_\infty = 0$, $f_r = 1300$ Hz, and $\alpha = 0.13$. The agreement is quite good. The BPLC sample 2 has a much lower relaxation frequency than that of sample 1 due to its larger $\varepsilon_{//}$ ($\sim$112) and $\Delta\varepsilon$ ($\sim$94). For this specific Chisso BPLC material, the strong frequency dependence of Kerr constant (from 120 Hz to 1 kHz) has to be taken into consideration when choosing a proper operation frequency for high speed photonic and display applications.

We also measured the temperature increase of sample 2 at different frequencies by attaching a thermocouple to the glass substrate. For easy comparison, we applied a constant voltage $50V_{rms}$ for all frequencies. The temperature was read after about an hour when the LC cell had reached its thermal equilibrium with the ambient. Figure 5 depicts the measured temperature raise. In general, as the frequency increases, the cell temperature increases because of dielectric heating of the LC material,[18,19] which is proportional to $2\pi f\varepsilon'' E^2$. For a given frequency, both imaginary part and voltage play important roles in dielectric heating. In an IPS cell, the electric fields are not uniform spatially, thus the quantitative explanation of the heating effect is difficult. From Fig. 5, as long as $f < 10$ kHz, the temperature increase is below 12°, which is still acceptable for most applications.

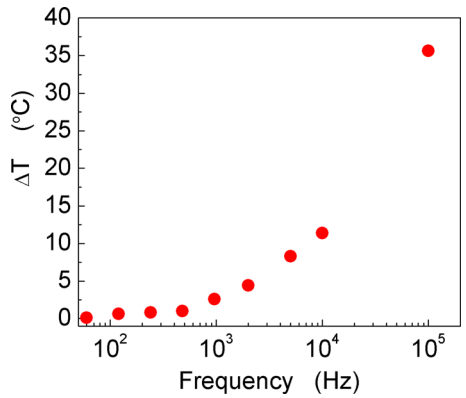

FIG. 5. (Color online) Measured temperature increase of sample 2 at different frequencies.

In conclusion, we have experimentally investigated the frequency effects on the Kerr constants of two polymer-stabilized BPLCs. As frequency increases, Kerr constant decreases gradually. This phenomenon can be described well by the extended Cole-Cole equation. We have also investigated the dielectric heating of Chisso JC-BP01M and found that the temperature increase is below 12 °C when the electric field frequency is below 10 kHz.

The authors are indebted to Jin Yan for technical assistance and Industrial Technology Research Institute (Taiwan) for financial support.

[1]H. Kikuchi, M. Yokota, Y. Hisakado, H. Yang, and T. Kajiyama, Nature Mater. **1**, 64 (2002).
[2]Y. Hisakado, H. Kikuchi, T. Nagamura, and T. Kajiyama, Adv. Mater. **17**, 96 (2005).
[3]For a review, J. Yan, J. Yan, L. Rao, M. Jiao, Y. Li, H. C. Cheng, and S. T. Wu, J. Mater. Chem. **21**, 7870 (2011).
[4]Z. Ge, S. Gauza, M. Jiao, H. Xianyu, and S. T. Wu, Appl. Phys. Lett. **94**, 101104 (2009).
[5]L. Rao, Z. Ge, S. T. Wu, and S. H. Lee, Appl. Phys. Lett. **95**, 231101 (2009).
[6]K. M. Chen, S. Gauza, H. Xianyu, and S. T. Wu, J. Display Technol. **6**, 49 (2010).
[7]D. P. Resler, D. S. Hobbs, R. C. Sharp, L. J. Friedman, and T. A. Dorschner, Opt. Lett. **21**, 689 (1996).
[8]Y. H. Lin, H. S. Chen, H. C. Lin, Y. S. Tsou, H. K. Hsu, and W. Y. Li, Appl. Phys. Lett. **96**, 113505 (2010).
[9]J. Yan, Y. Li, and S. T. Wu, Opt. Lett. **36**, 1404 (2011).
[10]M. Mori, T. Hatada, K. Ishikawa, T. Saishouji, O. Wada, J. Nakamura, and N. Terashima, J. Soc. Inf. Disp. **7**, 257 (1999).
[11]S. Gauza, X. Zhu, W. Piecek, R. Dabrowski, and S. T. Wu, J. Disp. Technol. **3**, 250 (2007).
[12]J. Yan, H. C. Cheng, S. Gauza, Y. Li, M. Jiao, L. Rao, and S. T. Wu, Appl. Phys. Lett. **96**, 071105 (2010).
[13]M. Jiao, J. Yan, and S. T. Wu, Phys. Rev. E **83**, 041706 (2011).
[14]L. Rao, J. Yan, S. T. Wu, S. Yamamoto, and Y. Haseba, Appl. Phys. Lett. **98**, 081109 (2011).
[15]P. R. Gerber, Mol. Cryst. Liq. Cryst. **116**, 197 (1985).
[16]K. S. Cole and R. H. Cole, J. Chem. Phys. **9**, 341 (1941).
[17]T. K. Bose, B. Campbell, S. Yagihara, and J. Thoen, Phys. Rev. A **36**, 5767 (1987).
[18]H. Xianyu, S. T. Wu, and C. L. Lin, Liq. Cryst. **36**, 717 (2009).
[19]A. C. Metaxas, and R.J. Meredith, *Industrial Microwave Heating* (IET, London, 1983).